Journal of Engineering Science and Technology
Vol. 16, No. 3 (2021) 2748 - 2762

EFFECTS OF SHAPE AND SKEW-ANGLE OF BRIDGE PIERS ON LOCAL SCOUR

ABDUL-HASSAN KH. AL-SHUKUR, NOOR SAADI HUSSEIN*

Department of Civil Engineering, Faculty of Engineering,
Babylon University, Babylon, 51001, Iraq
*Corresponding Author: noorsaadi2000@googlemail.com

Abstract

In this study, laboratory experiments were performed to evaluate the effects of shape and skewness-angle of bridge piers on the local scour. Experiments were carried out in the laboratory using a transparent rectangular flume with a steel frame structure flume. The experimental work has been carried out under clear-water conditions using three sets of piers (4 cm in width and 40 cm in length) arranged in one row with two different shapes (lenticular and oblong) and four different skewness-angles (α) (0°, 15°, 30°, 45°), while the ratio of the spacing between piers to the width pier was kept constant at 2. Additionally, the effects of flow velocity on the local scour were examined at three velocities, namely 0.17, 0.23, and 0.27 m/s. The flume bed was made from sand with average grain size (d50) of 0.71 mm, and a geometric standard deviation of 1.14. The obtained results showed that the depth of the local scour was significantly affected by all the studied parameters (skewness-angle, flow velocity, and shape of piers). The maximum scour depth (13.2 cm) was noticed in the lenticular piers when the skewness-angle and flow velocity were 30° and 0.27 m/s, while the lowest scour depth (1 cm) was noticed in the lenticular pier when the skewness-angle and flow velocity were 0° and 0.17 m/s, respectively.

Keywords: Clear water, Local scour, Piers shape, Skew angle.

1. Introduction

Scour is defined as normal event proceeds by the flow of water in rivers [1]. Local scour is one of the significant common threats to bridge foundations and piers, and this phenomenon is responsible for the majority of bridges failure worldwide [2]. For example, the literature shows that more than 130 bridges were failed in the USA between 1989 and 1999, and about 25% of the bridges in the USA are currently [3]. Similarly, 26% of the bridges in Canada are threatened [4]. In addition, expensive maintenance processes are required to avoid the whole failure of bridges due to the scouring phenomenon, for example, the recent literature indicated that the required cost to maintain about 11% of the total bridges in the USA is $76 billion [3; 4].

Bridge scour failure usually occurs in floods events when the overflow of rivers leads to changes in channel morphology, which in turn results in an uneven eroding of the sediments (usually consist of alluvial sand and stiff clay), and consequently weakens the foundations of the bridges and minimizes their load-carrying capacities [5]. When floods occur, water will decrease the level of the riverbed exposing the piers to harsh conditions. For example, decreasing the level of the riverbed leads to a significant loss in the load-carrying capacities of the piers due to the significant loss in the skin friction (between the soil and structure), which could result in structural failure [1]. The published literature confirmed that the intensity of the scouring phenomenon is not only related to the flow of rivers but also it is influenced by both shape of the piers and skewness-angle, where it has been reported that the skewness could result in a deep scour [6]. Thus, the mechanisms of the scouring phenomenon are complexed and depend on several factors. The depth of the scouring process depends on the characteristics of the flow, the bridge foundation geometry, and the characteristics of the riverbed soil (layering, grade, particle size, particle shape, and cohesion) [5].

Generally, the depth of local scour increases with the increase of the width of the pier, while the relationship between the depth of scour and the skewing-angle is complex due to the interactions between the width of the scour holes and the lateral expansion of the scouring. At skewed piers, the magnitudes of both scour expansions and the maximum depth of scouring (ds) depend on the angle of attack (α) because the flow area is influenced by the angle of attack. For example, Castiblanco [7] carried out a detailed study, involved 84 long-duration laboratory tests, about the scouring phenomenon at complex piers (complex geometry). This study examined the effects of the relative pier width, net pier hight, and the configuration pier groups on the scoring of 7 complex piers. The outcomes of their study indicated that the characteristics of the scouring processes are influenced by the depth, geometry, and configuration of piers, it was also found that flow regime influences the characteristics of the scouring process.

Ahmad et al. [8] investigated the mechanism of scour at a wide range of skewness-angle using two different types of uniform cohesionless bed sediment (d50 of 0.23 and 0.80 mm). The outcomes of their study indicated that the sour depth is a function of effects of the aspect ratios, the angles of attack (α), flow characteristics, nature of the bed materials, and the sediment gradation. A number of studies were focused on the effects of the pier shape and alignment on the scour depth, for example, Du and Liang [9] used two different shapes of piers (square and circular) to investigate the effects of piers shape on the scour depth considering the

effects centres of the upstream boundary and upstream corners. The obtained results indicated that the deepest scour was noticed near the circular piers, while the highest deposition rate was noticed near the square piers.

Günal et al. [10] studied the variation in the scour depths at a set of piers as a function of several factors, including the flow conditions, dimensions of piers, characteristics of the bed material, and distance between piers. The authors indicated that although the depth of scour was influenced by all the mentioned parameters, the span length has the most significant effect on the scour depth. Yang et al. [11] examined the combined effects of the skewness-angles (0°-90°), pile-cap and the pile group on the scouring of piers. The studied piers were divided into three groups according to the skewness-angle; aligned (0°), slight skewness (15°), and high skewness (more than 30°). The results revealed that increasing the skewness-angle minimized the effects of the pile-cap and the pile group.

Some of published literature focused on the relationship between the particle size and the scour depth, and also the relationship between the curveting degree of the channel and the scour depth. For example, Mahmoud [12] studied the scour depth as a function of the size of grains of soil downstream the piers in curved channels; the results obtained demonstrated that the minimum sour depth was obtained in soils with a grain size of 0.1-0.14 mm.

Helmy et al. [13] investigated the combined effects of the channel curveting degree and piers shape on the depth of the local scour. The outcomes of this study proved that the minimum scour depth, at a 30 degrees curved flume, was noticed around the lenticular piers due to the ability of this shape of piers to minimize the generation of horseshoe and the strength of vortices near the piers.

The above brief literature survey on the scour of piers revealed that it is a complex process and could result in grave consequences, such as the whole or partial failure of the bridges. Taking into accounts that the number of flood events and unexpected variations in rivers flow would dramatically increase within the next few decades due to global warming [14-21], and uneven distribution of rain water [22-28] that resulted from water pollution [29-35] and human activities [36-42], such as cement industry [43-50], concrete production [51-55], solid wastes accumulation [56-59], pollutants and other industries [60-66]. Thus, more studies on the scouring of bridges piers are required to have a better understanding of this phenomenon, and to avoid its grave consequences.

In this context, the present study aims at investigating the combined effects of skewness-angle, the ratio of the spacing between piers to the width pier, and flow velocity on the depth of local scour by carrying a series of experiments under clear water conditions and uniform bed material. Thus, the outcomes of this study could be a preliminary guideline for researchers and engineers about the effects of the mentioned parameters on the intensity of the scouring process.

2. Laboratory Flume

Experiments were carried out using a rectangular recirculation flume, which has transparent walls with a steel frame structure with net dimensions of 7.5 m in length, 1 m in width, and 0.6 m in depth. A cavity section, 2 m in length, and 0.2 m in depth, was located at 2.5 m from the flume inlet section (upstream). This cavity has been filled with sand (with an average grain size (d50) of 0.71 mm). Two

overhead tanks (1×0.9×0.55) were installed at the upstream side of the flume to supply a continuous flow, and another two tanks (1×0.9×0.55) were installed at the end of the flume (ground tanks) to collect the used water.

The used water was circulated between the overhead and ground tanks using a water pump (with a maximum pumping capacity of 13.3 L/s). A wooden gate (as a suppressor) was installed at the beginning (upstream) of the flume to smooth the flow coming onto the sand bed, and two screens' baffles were installed at 50 cm-intervals from the flume inlet to damp any turbulence and to smooth the flow to prevent any undesired bedform (ripple or dune) at the working section. To control the velocity of flow and the depth of water at the end of the flume, a rectangular gate (1×1 m) has been installed at the outlet of the flume.

A flow meter has been utilized (with an accuracy of 0.004) at the return pipe) to measure the water discharge. Additionally, a mobile point gauge that is mounted on a brass rail at the top of the flume was used to measure the depths. It is noteworthy to highlight that all dimensions and specifications used in this study were selected to be within the published literature [2].

3. Model of Bridge Piers

As it has been mentioned that the main goal of the present study is the examination of the effects of piers shape (lenticular and oblong), skewness-angles (0°, 15°, 30°, 45°), and flow velocity on the local scour. To achieve this goal, steel piers have been manufactured in the laboratories of the civil engineering department, university of Babylon, Iraq. The net dimensions of the manufacture piers were 40 cm in length and 4 cm in width (maximum width), as shown in Fig. 1. These dimensions were selected following the literature to avoid the influence of contraction on the depth of the local scour.

Fig. 1. Piers shapes.

In each run, three piers from each type were arranged in one row in the flume, and the flow direction was changed according to the required skewness angle.

4. Dimensional Analysis

To have a better understanding about both scour mechanism and effects of the studied parameters on the scour depth, a wide range of parameters have included in

this investigation, including the scour depth (*ds*), piers width (*Dp*), water depth (*d*), flow velocity (*V*), the critical velocity (*Vc*), sediment size (*d50*), duration of flow (*T*), pier shape factor (*Ks*), alignment coefficient ($K\alpha$), the spacing of piers (*S*), skewness-angle (α), number of piers (*m*), flume width (*B*), gravitational acceleration (*g*), length of the pier (*L*), fluid density (ρ), sediment density (ρs), angle of static sediment ($\emptyset$), dynamic viscosity fluid (μ), slope of channel bed (*So*) and laboratory temperature (θ). These parameters could be summarised using the following equation:

$$ds/Dp = f\,(Vc/V, \alpha, L/Dp, V2/gDp, K\alpha) \quad (1)$$

5. Experimental Procedures

The experimental work was carried out as follows:

- Initially, the piers were installed in the flume at the required position (vertically or with the skewness-angles).
- The bed material (sand) with a mean particle size (d50) of 0.71mm was placed in the cavity and manually levelled using a scraper. The elevation of the bed surface was checked at random points, using the point gauge. The thickness of the sand layer was 20 cm.
- The flume was gradually filled with water to the required depth, 5 cm. The flume was carefully filled to avoid the destruction of sediment.
- The water pumping process (circulation) was started at low speed and gradually increased unit the desire flow rate was attained to avoid the destruction of sediment; the tailgate was checked to maintain the correct depth of flow in the flume.
- At the end of the testing time, which was monitored using a stopwatch, the flow was stopped, and the water was carefully drained from the flume. Then the depth and location of the maximum scour were recorded. The maximum depth of scour was measured at 2 minutes-intervals for the first hour of experiments, then at 10-minutes intervals for the rest of the time (5 hours).
- The experiments were repeated by re-levelling the surface of the sand (bed of the flume), and the same steps above were repeated.
- The above steps were used to check the effects of each one of the studied parameters (shape of pier, skewness-angle, and velocity of the flow).

Table 1 summarized the experimental conditions

Table 1. Experimental conditions.

No.	Flow intensity	*Y* (m)	Velocity in the flume (m/s)	*Q* (L/s)	Fr	Re
1	0.6	0.05	0.17	8.5	0.243	13770
2	0.8	0.05	0.23	11.5	0.328	18630
3	0.95	0.05	0.27	13.3	0.386	21870

6. Results

To examine the effects of the piers shape, three piers of each shape of piers (lenticular and oblong piers) were arranged in one row (perpendicular to the flow direction, α= 0^o), see Figs. 2 and 3, and subjected to three flow intensities (*V/Vc*) (0.6, 0.8, and

0.95). The ratio of the spacing between piers to the diameter of the pier (S/D_p) was kept constant at 2 for all experiments.

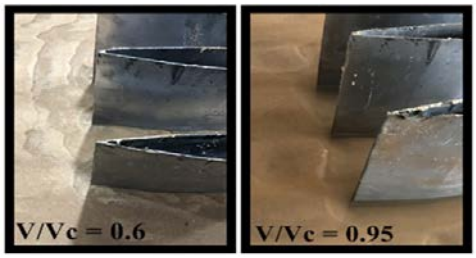

Fig. 2. Scour pattern after six hours of flow for lenticular piers.

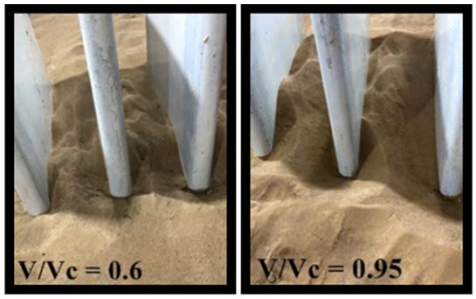

Fig. 3. Scour pattern after six hours of flow for oblong piers.

The obtained results from the lenticular shape, as shown in Fig. 4, indicated that the scour depth has increased from 1, 2.4 to 4.1 cm when the flow intensity increased from 0.17, 0.23 to 0.27 m/s, respectively. Figure 4 also shows the variation of scour depth, at the lenticular piers, with the flow time for each one the studied flow intensity. It can be seen from this figure that about 75% of scour depth is achieved within the first 50 minutes.

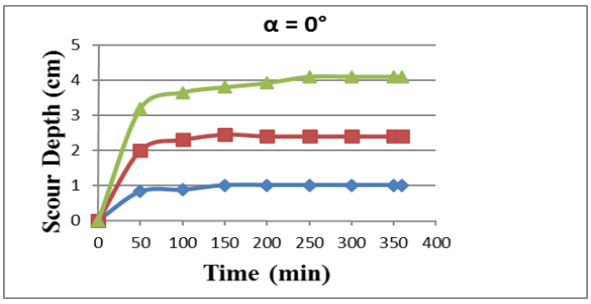

Fig. 4. Scour variation with time at different flow intensities.

The same trend was noticed in the oblong piers. Generally, the performance of the lenticular, in terms of scour depth, piers was better than that of the oblong ones, which could be attributed to the fact that the geometry of the lenticular piers substantially minimizes the formation of a horseshoe and wakes the generated vortices and consequently minimizes the scour depth [13]. Additionally, it was

noticed that maximum scour depth occurred at about 2/3 of the lenticular pier width from the upstream side that could be attributed to the effects of contraction of the area and formation of horizontal velocity jet. The relevant literature showed comparable results [67].

Then, the effects of the skewness-angles (at 0°, 15°, 30°, and 45°) on the scouring depth was investigated using the same procedures stated in the previous experiments. The obtained results, Fig. 5, indicated that increasing the skewness-angle has increased the depth of the sour for the range from 0° to 30°, then the scour depth decreased when the skewness-angle increased from 30° to 45°, see fig. 5.

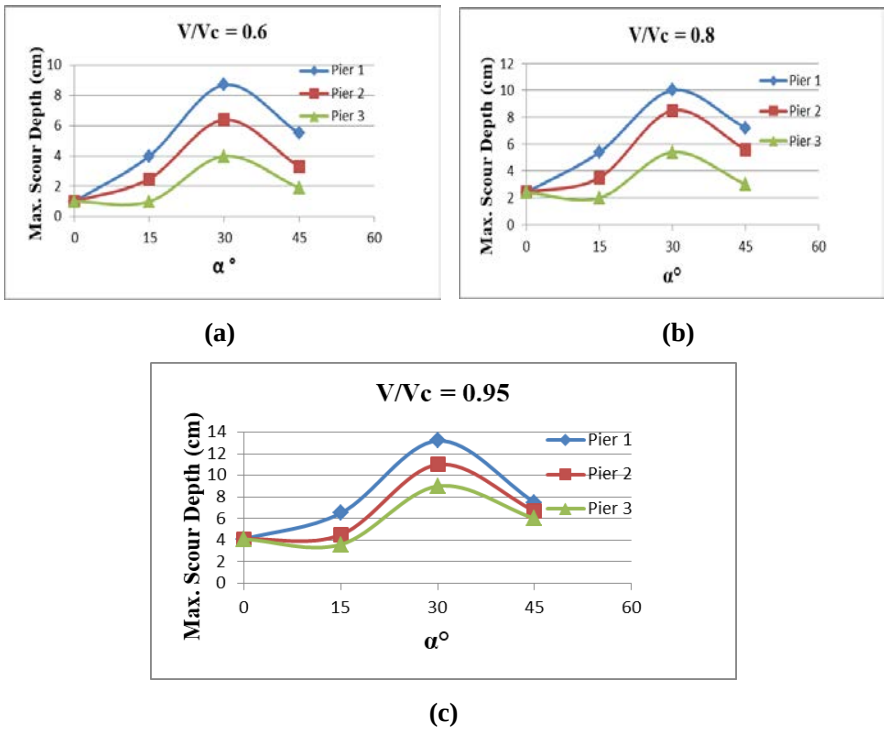

Fig. 5. Comparison between the depth of scour and skewness-angle.

The same experiments were repeated for the oblong shape. The obtained results are listed in Table 2. Generally, the results obtained indicated that the maximum scour depth (13.2 cm) happened at the oblong piers when the skewness-angle was 30° and at the maximum flow intensity (0.95). Similar results were found by many previous studies [68].

It can be noticed from Table 2 that the lenticular pier has the best resistance for the local scour that could be attributed to the fact that this shape of piers has the minimum exposure area, which minimizes the occurrence of the horseshoe vortices (the main cause of local scour). Similar results were found in the literature [2].

In summary, the obtained results indicated that all the studied parameters have significant effects on the scour depth. Additionally, it has been found that the scour depth could be minimized by adopting the lenticular piers and keeping the flow intensity

and skewness-angle as low as possible. Also, scouring depth could be monitored using advanced sensing technologies such as electromagnetic sensors [69-73].

Table 2. Experimental data.

No.	Shape	$\alpha°$	Q (L/s)	V (m/s)	Vc (m/s)	V/Vc	Max. Scour depth (cm)		
							P1	P2	P3
1	Lenticular	0	8.5	0.17	0.283	0.6	1	1	1
2	Lenticular	0	11.5	0.23	0.283	0.8	2.4	2.4	2.4
3	Lenticular	0	13.3	0.27	0.283	0.95	4.1	4.1	4.1
4	Lenticular	15	8.5	0.17	0.283	0.6	4	2.5	1
5	Lenticular	15	11.5	0.23	0.283	0.8	5.4	3.5	2
6	Lenticular	15	13.3	0.27	0.283	0.95	6.5	4.5	3.6
7	Lenticular	30	8.5	0.17	0.283	0.6	8.7	6.4	4
8	Lenticular	30	11.5	0.23	0.283	0.8	10	8.5	5.4
9	Lenticular	30	13.3	0.27	0.283	0.95	11	11	9
10	Lenticular	45	8.5	0.17	0.283	0.6	5.5	3.3	1.9
11	Lenticular	45	11.5	0.23	0.283	0.8	7.2	5.6	3
12	Lenticular	45	13.3	0.27	0.283	0.95	7.5	6.7	6
13	Oblong	0	8.5	0.17	0.283	0.6	3.1	3.1	3.1
14	Oblong	0	11.5	0.23	0.283	0.8	5	5	5
15	Oblong	0	13.3	0.27	0.283	0.95	6.1	6.1	6.1
16	Oblong	15	8.5	0.17	0.283	0.6	6.5	4.7	3.8
17	Oblong	15	11.5	0.23	0.283	0.8	7.4	6.5	5.4
18	Oblong	15	13.3	0.27	0.283	0.95	9	7.6	6.6
19	Oblong	30	8.5	0.17	0.283	0.6	8.4	6.1	3.8
20	Oblong	30	11.5	0.23	0.283	0.8	9.3	8	5.2
21	Oblong	30	13.3	0.27	0.283	0.95	13.2	9.4	8.8
22	Oblong	45	8.5	0.17	0.283	0.6	6	4.6	3
23	Oblong	45	11.5	0.23	0.283	0.8	9.2	8	5.1
24	Oblong	45	13.3	0.27	0.283	0.95	10.8	9.2	7.8

7. Conclusions

The following is the conclusions extracted from this research:

- For all experiments, the deepest scour occurs at the pier near the abutment at upstream.
- The scour depth increases with the increase of the flow intensity.
- The equilibrium scour depth and first scour rate depend on the shape of the pier and skewness-angle.
- The lenticular pier has good protection against the local scour because of its low exposure area and geometry that prevents the formation of the horseshoe.
- The lenticular shape is considered the best shape of piers as it minimizes the scour depth by 30% in comparison with the oblong shape.

Acknowledgments

The authors wish to express their gratitude and sincere appreciation to the staff of the construction laboratory at the civil engineering department, university of Babylon, for their assistance in providing a place to set up the flume.

Nomenclatures

D_p	Width of bridge pier, cm
d_{50}	Median grain size of sediment, mm
ds	Maximum scour depth, cm
Fr	Froude Number
P1	Pier number one
P2	Pier number two
P3	Pier number three
Q	Total discharge, m^3/sec
Re	Reynolds number
S	Spacing among piers, cm
V/Vc	Flow intensities
V	Mean velocity of approach flow, m/s
Vc	Mean velocity at threshold motion of sediment for approach flow, m/s
Y	Depth of flow, cm

Greek Symbols

α	Skewness-angle, degree
σ_g	Geometric standard deviation of sediment

References

1. Das, S.; Das, R.; and Mazumdar, A. (2014). Variations in clear water scour geometry at piers of different effective widths. *Turkish Journal of Engineering and Environmental Sciences*, 38(1), 97-111.
2. Vijayasree, B.; Eldho, T.I.; Mazumder, B.S.; and Ahmad, N. (2019). Influence of bridge pier shape on flow field and scour geometry. *International Journal of River Basin Management*, 17(1), 109-129.
3. Bazzucchi, F.; Restuccia, L.; and Ferro, G.A. (2018). Considerations over the Italian road bridge infrastructure safety after the Polcevera viaduct collapse: past errors and future perspectives. *Frattura e Integrita Strutturale*, 12(46), 400-421.
4. Omar, T.; and Nehdi, M.L. (2018). Condition assessment of reinforced concrete bridges: Current practice and research challenges. *Infrastructures*, 3(3), 36.
5. Akhlaghi, E.; Babarsad, M.S.; Derikvand, E.; and Abedini, M. (2020). Assessment the effects of different parameters to rate scour around single piers and pile groups: A review. *Archives of Computational Methods in Engineering*, 27(1), 183-197.
6. Yang, Y.; Melville, B.W.; Macky, G.H.; and Shamseldin, A.Y. (2019). Local scour at complex bridge piers in close proximity under clear-water and live-bed flow regime. *Water*, 11(8), 1530.
7. Castiblanco, M.E. (2016). *Experimental study of local scour around complex bridge piers.* Ph.D. Thesis, Civil Engineering Department University of Porto, Portugal.
8. Ahmad, N.; Melville, B.; Mohammad, T.; Ali, F.; and Yusuf, B. (2017). Clear-water scour at long skewed bridge piers. *Journal of the Chinese Institute of Engineers*, 40(1), 10-18.

9. Du, S.; and Liang, B. (2019). Comparisons of local scouring for submerged square and circular cross-section piles in steady currents. *Water*, 11(9), 1820.
10. Günal, M.; Gelmeran, T.A.; and Günal, A. (2017). Local scour around group bridge pier with different shapes. *Acta Physica Polonica Series A*, 132(3), 632-633.
11. Yang, Y.; Melville, B.W.; Sheppard, D.M.; and Shamseldin, A.Y. (2018). Clear-water local scour at skewed complex bridge piers. *Journal of Hydraulic Engineering*, 144(6), 1-8.
12. Mahmoud, A.H. (2020). Effect of soil particle size in reducing the scour around bridge piers at the curved channels. *Life Science Journal*, 17(4), 43-49.
13. Helmy, A.; Ali, M.; and Ahmed, H. (2017). An experimental study of local scour around piers in the curved channels. *Journal of Multidisciplinary Engineering Science and Technology*, 4(1), 6448-6453.
14. Zubaidi, S.L.; Kot, P.; Hashim, K.S.; AlKhaddar, R.; Abdellatif, M.; and Muhsin, Y.R. (2019). Using LARS-WG model for prediction of temperature in Columbia City, USA. *Proceedings of the IOP Conference Series: Materials Science and Engineering*, 584, 012026.
15. Zubaidi, S.L.; Ortega-Martorell, S.; Al-Bugharbee, H.; Olier, I.; Hashim, K.S.; Gharghan, S.K.; Kot, P.; and AlKhaddar, R. (2020). Urban water demand prediction for a city that suffers from climate change and population growth: Gauteng province case study. *Water*, 12(7), 1885.
16. Zubaidi, S.L.; Al-Bugharbee, H.; Muhsen, Y.R.; Hashim, K.S.; AlKhaddar, A..; and Hmeesh, W.H. (2019). The prediction of municipal water demand in Iraq: A case study of Baghdad governorate. *Proceedings of the 12th International Conference on Developments in eSystems Engineering (DeSE)*, Kazan, Russia, 274-277.
17. Zubaidi, S.L; Hashim, K.S.; Ethaib, S.; Al-Bdairi, N.S.S.; Al-Bugharbee, H.; and Gharghan, S.K. (in press). A novel methodology to predict monthly municipal water demand based on weather variables scenario. *Journal of King Saud University-Engineering Sciences*.
18. Hashim, K.S.; Ali, S.S.M.; AlRifaie, J.K.; Kot, P.; Shaw, A.; AlKhaddar, R.; Idowu, I.; and Gkantou, M. (2020). Escherichia coli inactivation using a hybrid ultrasonic–electrocoagulation reactor. *Chemosphere*, 247, 125868.
19. Hashim, K.S.; AlKhaddar, R.; Shaw, A.; Al-Jumeily, D.; Alwash, R.; and Aljefery, M.H. (2020). *Electrocoagulation as an eco-friendly River water treatment method. In Advances in Water Resources Engineering and Management*. Berlin: Springer.
20. Al-Jumeily, D.; Alwash, R.; and Aljefery, M.H. (2020). Electrocoagulation as an eco-friendly River water treatment method. *Advances in Water Resources Engineering and Management*): Springer, 219-235.
21. Hashim, K.S.; Ewadh, H.M.; Muhsin, A.A.; Zubaidi, S.L.; Kot, P.; Muradov, M.; Aljefery, M.; and AlKhaddar, R. (2020). Phosphate removal from water using bottom ash: Adsorption performance, coexisting anions and modelling studies. *Water Science and Technology*, 83(1), 77-89.
22. Zubaidi, S.L.; Al-Bugharbee, H.; Ortega-Martorell, S.; Gharghan, S.; Olier, I.; Hashim, K.S.; Al-Bdairi, N.S.S.; and Kot, P. (2020). A novel methodology for prediction urban water demand by wavelet denoising and adaptive neuro-fuzzy inference system approach. *Water*, 12(6), 1628.

23. Zanki, A.K.; Mohammad, F.H.; Hashim, K.S.; Muradov, M.; Kot, P.; Kareem, M.M.; and Abdulhadi, B. (2020). Removal of organic matter from water using ultrasonic-assisted electrocoagulation method. *Proceedings of the IOP Conference Series: Materials Science and Engineering*, 888, 012033.
24. Zubaidi, S.L.; Al-Bugharbee, H.; Muhsin, Y.R.; Hashim, K.S.; and AlKhaddar, R. (2020). Forecasting of monthly stochastic signal of urban water demand: Baghdad as a case study. *Proceedings of the IOP Conference Series: Materials Science and Engineering*, 888, 012018.
25. Zubaidi, S.L.; Abdulkareem, I.H.; Hashim, K.S.; Al-Bugharbee, H.; Ridha, H.M.; Gharghan, S.K.; Al-Qaim, F.F.; Muradov, M.; Kot, P.; and AlKhaddar, R. (2020). Hybridised artificial neural network model with slime mould algorithm: A novel methodology for prediction urban stochastic water demand. *Water*, 12(10), 2692.
26. Al-Naimi, H.; Idan, I.J.; Al-Janabi, A.; Hashim, K.S.;, Gkantou, M.; Zubaidi, S.L.; Kot, P.; and Muradov, M. (2020). Ultrasonic-electrochemical treatment for effluents of concrete plants Ultrasonic-electrochemical treatment for effluents of concrete plants. *Proceedings of the IOP Conference Series: Materials Science and Engineering*, 888, 012063.
27. Abdulhadi, B.; Kot, P.; Hashim, K.S.; Shaw, A.; Muradov, M.; and AlKhaddar, A. (2021). Continuous-flow electrocoagulation (EC) process for iron removal from water: Experimental, statistical and economic study. *Science of The Total Environment*, 760, 143417.
28. Hashim, K.S.; Shaw, A.; AlKhaddar, R.; Kot, P.; Al-Shamma'a, A. (2021). Water purification from metal ions in the presence of organic matter using electromagnetic radiation-assisted treatment. *Journal of Cleaner Production*, 280(Part 2), 124427.
29. Hashim, K.S.; Hussein, A.H.; Zubaidi, S.L.; Kot, P.; Kraidi, L.; AlKhaddar, R.; Shaw, A.; and Alwash, R. (2019). Effect of initial pH value on the removal of reactive black dye from water by electrocoagulation (EC) method. *Proceedings of the IOP Conference Series*: *Journal of Physics: Conference Series*, 1294, 072017.
30. Hashim, K.S.; AlKhaddar, R.; Jasim, N.; Shaw, A.; Phipps, D.; Kot, P.; Pedrola, M.O.; Alattabi, A.W.; Abdulredha, M.; and Alawsh, R. (2019). Electrocoagulation as a green technology for phosphate removal from river water. *Separation and Purification Technology*, 210, 135-144.
31. Abdulraheem, F.S.; Al-Khafaji, Z.S.; Hashim, K.S.; Muradov, M.; Kot, P.; and Shubbar, A.A. (2020). Natural filtration unit for removal of heavy metals from water. *Proceedings of the IOP Conference Series: Materials Science and Engineering*, 888, 012034.
32. Alenazi, M.; Hashim, K.S.; Hassan, A.A.; Muradov, M.; Kot, P.; and Abdulhadi, B. (2020). Turbidity removal using natural coagulants derived from the seeds of strychnos potatorum: statistical and experimental approach. *Proceedings of the IOP Conference Series: Materials Science and Engineering*, 888, 012064.
33. Alenezi, A.K.; Hasan, H.A.; Hashim, K.S.; Amoako-Attah, J.; Gkantou, M.; Muradov, M.; Kot, P.; and Abdulhadi, B. (2020). Zeolite-assisted electrocoagulation for remediation of phosphate from calcium-phosphate

solution. *Proceedings of the IOP Conference Series: Materials Science and Engineering*, 888, 012031.

34. Alhendal, M.; Nasir, M.J.; Hashim, K.S.; Amoako-Attah, J.; Al-Faluji, D.; Muradov, M.; Kot, P.; and Abdulhadi, B. (2020). Cost-effective hybrid filter for remediation of water from fluoride. *Proceedings of the IOP Conference Series: Materials Science and Engineering*, 888, 012038.
35. Al-Marri, S.; AlQuzweeni, S.S.; Hashim, K.S.; AlKhaddar, R.; Kot, P.; AlKizwini, R.S.; Zubaidi, S.L.; and Al-Khafaji, Z.S. (2020). Ultrasonic-Electrocoagulation method for nitrate removal from water. *Proceedings of the IOP Conference Series: Materials Science and Engineering*, 888, 012073.
36. Alattabi, A.W.; Harris, C.; AlKhaddar, R.; Alzeyadi, A.; and Hashim, K.S. (2017). Treatment of residential complexes' wastewater using environmentally friendly technology. *Procedia Engineering*, 196, 792-799.
37. Alattabi, A.W.; Harris, C.B.; AlKhaddar, R.M.; Hashim, K.S.; Ortoneda-Pedrola, M.; and Phipps, D. (2017). Improving sludge settleability by introducing an innovative, two-stage settling sequencing batch reactor. *Journal of Water Process Engineering*, 20, 207-216.
38. Hashim, K.S.; Shaw, A.; AlKhaddar, R.; Ortoneda Pedrola, M.; and Phipps, D. (2017). Defluoridation of drinking water using a new flow column-electrocoagulation reactor (FCER) - Experimental, statistical, and economic approach. *Journal of Environmental Management*, 197, 80-88.
39. Hashim, K.S.; Shaw, A.; AlKhaddar, R.; Ortoneda Pedrola, M.; and Phipps, D. (2017). Iron removal, energy consumption and operating cost of electrocoagulation of drinking water using a new flow column reactor. *Journal of Environmental Management*, 189, 98-108.
40. Hashim, K.S.; Shaw, A.; AlKhaddar, R.; Ortoneda Pedrola, M.; and Phipps, D. (2017). Energy efficient electrocoagulation using a new flow column reactor to remove nitrate from drinking water - Experimental, statistical, and economic approach. *Journal of Environmental Management*, 196, 224-233.
41. Hashim, K.S.; Al-Saati, N.H.; Hussein, A.H.; and Al-Saati, Z.N. (2018). An investigation into the level of heavy metals leaching from canal-dreged sediment: A case study metals leaching from dreged sediment. *Proceedings of the IOP Conference Series: Materials Science and Engineering*, 454, 012022
42. Hashim, K.S.; Idowu, I.A.; Jasim, N.; AlKhaddar, R.; Shaw, A.; Phipps, D.; Kot, P.; Ortoneda Pedrola, M.; Alattabi, A.W.; Abdulredha, M.; Alwash, R.; Teng, K.H.; Joshi, K.H.; and Aljefery, M.H. (2018). Removal of phosphate from River water using a new baffle plates electrochemical reactor. *MethodsX*, 5, 1413-1418.
43. Majdi, H.S.; Shubbar, A.A.; Nasr, M.S.; Al-Khafaji, Z.S.; Jafer, H.; Abdulredha, M.; Al Masoodi, Z.; Sadique, M.; and Hashim, K.S. (2020). Experimental data on compressive strength and ultrasonic pulse velocity properties of sustainable mortar made with high content of GGBFS and CKD combinations. *Data in Brief*, 31, 105961.
44. Shubbar, A.A.; Sadique, M.; Nasr, M.S.; Al-Khafaji, Z.S. ; and Hashim, K.S. (2020). The impact of grinding time on properties of cement mortar incorporated high volume waste paper sludge ash. *Karbala International Journal of Modern Science*, 6(4), 396-403.

45. Shubbar, A.A.; Sadique, M.; Shanbara, H.K.; and Hashim, K.S. (2020). *The development of a new low carbon binder for construction as an alternative to cement.* In *Advances in sustainable construction materials and geotechnical engineering* (1st ed.). Berlin: Springer.
46. Emamjomeh, M.M.; Kakavand, S.; Jamali, H.A.; Alizadeh, S.M.; Safdari, M.; Mousavi, S.E.S.; Hashim, K.S.; and Mousazade, M. (2020). The treatment of printing and packaging wastewater by electrocoagulation–flotation: the simultaneous efficacy of critical parameters and economics. *Desalination and water treatment*, 205, 161-174.
47. Hashim, K.S.; Kot, P.; Zubaidi, S.L.; Alwash, R.; AlKhaddar, R.; Shaw, A.; Al-Jumeily, D.; and Aljefery, M.H. (2020). Energy efficient electrocoagulation using baffle-plates electrodes for efficient *Escherichia coli* removal from wastewater. *Journal of Water Process Engineering*, 33, 101079.
48. Aqeel, K.; Mubarak, H.A.; Amoako-Attah, J.; Abdul-Rahaim, L.A.; Al Kaddar, R.; Abdellatif, M.; Al-Janabi, A.; and Hashim, K.S. (2020). Electrochemical removal of brilliant green dye from wastewater. *Proceedings of the IOP Conference Series: Materials Science and Engineering*, 888, 012036.
49. Emamjomeh, M.M.; Mousazadeh, M.; Mokhtari, N.; Jamali, H.A.; Makkiabadi, M.; Naghdali, Z.; Hashim, K.S.; and Ghanbari, R. (2020). Simultaneous removal of phenol and linear alkylbenzene sulfonate from automotive service station wastewater: Optimization of coupled electrochemical and physical processes. *Separation Science and Technology*, 55(17), 3184-3194.
50. Al-Housni, M.; Hussein, A.H.; Yeboah, D.; AlKhaddar, R.; Abdulhadi, B.; Shubbar, A.A.; and Hashim, K.S. (2020). Electrochemical removal of nitrate from wastewater. *Proceedings of the IOP Conference Series: Materials Science and Engineering*, 888, 012037.
51. Kadhim, A.; Sadique, M.; Al-Mufti, R.; and Hashim, K.S. (2020). Long-term performance of novel high-calcium one-part alkali-activated cement developed from thermally activated lime kiln dust. *Journal of Building Engineering*, 32, 1-17.
52. Kadhim, A.; Sadique, M.; and Al-Mufti, R. (2020). Developing one-part alkali-activated metakaolin/natural pozzolan Binders using lime waste as activation Agent. *Advances in Cement Research*, 32(11), 1-38.
53. Al-Jumeily, D.; Hashim, K.S.; Alkaddar, R.; Al-Tufaily, M.; and Lunn, J. (2019). Sustainable and environmentally friendly ancient reed houses (Inspired by the past to motivate the future). *Proceedings of the 11th International Conference on Developments in eSystems Engineering (DeSE)*, Cambridge, UK, 214-219.
54. Shubbar, A.A.; Al-Shaer, A.; AlKizwini, R.S.; Al Hawesah, H.; and Sadique, M. (2019). Investigating the influence of cement replacement by high volume of GGBS and PFA on the mechanical performance of cement mortar. *Proceedings of the IOP Conference Series: Materials Science and Engineering*, 584, 012022.
55. Alyafei, A.; AlKizwini, R.S.; Hashim, K.S.; Yeboah, D.; Gkantou, M.; AlKhaddar, R.; Al-Faluji, D.; and Zubaidi, S.L. (2020). Treatment of effluents of construction industry using a combined filtration-electrocoagulation

method. *Proceedings of the IOP Conference Series: Materials Science and Engineering*, 012032.

56. Abdulredha, M.; AlKhaddar, R.; Jordan, D.; and Hashim, K.S. (2017). The development of a waste management system in Kerbala during major pilgrimage events: determination of solid waste composition. *Procedia Engineering*, 196, 779-784.
57. Abdulredha, M.; AlKhaddar, R.; Jordan, D.; Kot, P.; Abdulridha, A.; and Hashim, K.S. (2018). Estimating solid waste generation by hospitality industry during major festivals: A quantification model based on multiple regression. *Waste Management*, 77, 388-400.
58. Idowu, I.A.; Atherton, W.; Hashim, K.S.; Kot, P.; AlKhaddar, R.; Alo, B.I.; and Shaw, A. (2019). An analyses of the status of landfill classification systems in developing countries: Sub Saharan Africa landfill experiences. *Waste Management*, 87, 761-771.
59. Hashim, K.S.; Al-Saati, N.H.; Alquzweeni, S.S.; Zubaidi, S.L.; Kot, P.; Kraidi, L.; Hussein, A.H.; AlKhaddar, R.; Shaw, A.; and Alwash, R. (2019). Decolourization of dye solutions by electrocoagulation: an investigation of the effect of operational parameters. *IOP Conference Series: Materials Science and Engineering*, 584, 012024.
60. Grmasha, R.A.; Al-Sareji, O.J.; Salman, J.M.; and Hashim, K.S. (2020). Polycyclic aromatic hydrocarbons (PAHs) in urban street dust within three land-uses of Babylon Governorate, Iraq: Distribution, sources, and health risk assessment. *Journal of King Saud University - Engineering Sciences*, 33, 1-18.
61. Shubbar, A.A.; Jafer, H.; Dulaimi, A.; Hashim, K.S.; Atherton, W.; and Sadique, M. (2018). The development of a low carbon binder produced from the ternary blending of cement, ground granulated blast furnace slag and high calcium fly ash: An experimental and statistical approach. *Construction and Building Materials*, 187, 1051-1060.
62. Abdulla, G.; Kareem, M.M.; Hashim, K.S.; Muradov, M.; Kot, P.; Mubarak, H.A.; Abdellatif, M.; and Abdulhadi, B. (2020). Removal of iron from wastewater using a hybrid filter. *Proceedings of the IOP Conference Series: Materials Science and Engineering*, 888, 012035.
63. Abdulhadi, B.; Kot, P.; Hashim, K.S.; Shaw, A.; Muradov, M.; and AlKhaddar, R. (2020). Continuous-flow electrocoagulation (EC) process for iron removal from water: Experimental, statistical and economic study. *Science of The Total Environment*, 760, 143417.
64. Abdulhadi, B.A.; Kot, P.; Hashim, K.S.; Shaw, A.; and AlKhaddar, R. (2019). Influence of current density and electrodes spacing on reactive red 120 dye removal from dyed water using electrocoagulation/electroflotation (EC/EF) process. *IOP Conference Series: Materials Science and Engineering*, 854, 012035.
65. Al-Saati, N.H.; Hussein, T.K.; Abbas, M.H.; Hashim , K.; Al-Saati, Z.N.; Kot. P.; Sadique, M.; Aljefery, M.H.; and Carnacina, I. (2019). Statistical modelling of turbidity removal applied to non-toxic natural coagulants in water treatment: A case study. *Desalination and Water Treatment*, 150, 406-412.
66. Omran, I.I.; Al-Saati, N.H.; Hashim, K.S.; Al-Saati, Z.N.; Kot, P.; AlKhaddar, R.; Al-Jumeily, D.; Shaw, A.; Ruddock, F.; and Aljefery, M. (2019).

Assessment of heavy metal pollution in the Great Al-Mussaib irrigation channel. *Desalination and Water Treatment*, 168, 165-174.

67. Al-Quraishi, Z.A. (2016). *Effect of Bridge pier shape on the depth and configuration of local scour*. MSc. Thesis, College of Engineering, University of Babylon, Iraq.
68. Gooda, E.A.M.; Ettema, R.; Yassin, A.; and Melville, B.W. (2016). Simplified approach for the prediction of maximum equilibrium scour. *Alexandria Engineering Journal*, 35(2), 1-10.
69. Gkantou, M.; Muradov, M.; Kamaris, G.S.; Hashim, K.S.; Atherton, W.; and Kot, P. (2019). Novel electromagnetic sensors embedded in reinforced concrete beams for crack detection. *Sensors*, 19(23), 5175-5189.
70. Ryecroft, S.; Shaw, A.; Fergus, P.; Kot, P.; Hashim, K.S.; Moody, A.; and Conway, L. (2019). A first implementation of underwater communications in raw water using the 433 MHz frequency combined with a bowtie antenna. *Sensors*, 19(8), 1813-1823.
71. Ryecroft, S.P.; Shaw, A.; Fergus, P.; Kot, P.; Hashim, K.S.; Conway, L.; Moody, A. (2019). A novel gesomin detection method based on microwave spectroscopy. *Proceedings of the 12th International Conference on Developments in eSystems Engineering (DeSE)*, Kazan, Russia, 429-433.
72. Teng, K.H.; Kot, P.; Muradov, M.; Shaw, A.; Hashim, K.S.; Gkantou, M.; and Al-Shamma'a, A. (2019). Embedded smart antenna for non-destructive testing and evaluation (NDT&E) of moisture content and deterioration in concrete. *Sensors*, 19(3), 547-559.
73. Omer, G.; Kot, P.; Atherton, W.; Muradov, M.; Gkantou, M.; Shaw, A.; Riley, M.; Hashim, K.S.; and Al-Shamma'a, A. (2020). A non-destructive electromagnetic sensing technique to determine chloride level in maritime Concrete. *Karbala International Journal of Modern Science*, 6(4), 1-14.